

Comparison of Attitude Estimation Methods for Underwater Navigation

Nak Yong Ko

Dept. Electronic Engineering, Chosun University, Gwangju, Korea

Email: nyko@chosun.ac.kr

Seokki Jeong

Dept. Control and Instrumentation Engineering, Chosun University, Gwangju, Korea

Email: Seak-ki@hanmail.net

Hyun-Taek Choi

Korea Institute of Ocean Science and Technology, Daejeon, Korea

Email: htchoi@kriso.re.kr

Yong Seon Moon

Dept. Electronic Engineering, Sunchon National University, Sunchon, Korea

Email: moon@urc.com

Abstract—This paper compares attitude estimation methods that use microelectromechanical systems–attitude heading reference system (MEMS-AHRS) for underwater vehicle (UV) navigation. Although MEMS-AHRS is a cheap, lightweight, small, and easy-to-use instrument for attitude determination, the yaw estimate using the AHRS is not as reliable as the estimates of roll and pitch. This is because yaw estimation depends primarily on the magnetic field measurement, and the magnetic field measurement of the AHRS is vulnerable to magnetic interference induced by the vehicle and instrument itself and the environment surrounding the vehicle. This paper compares four major approaches: nonlinear explicit complementary filter (NECF), extended Kalman filter (EKF), sine rotation vector (SRV) method, and complementary filter (CF). The methods are tested through experiments in a test tank. The results show that the errors in yaw show notable differences between the methods. NECF and SRV show an improvement over the EKF and CF. This paper provides a practical comparison of the underwater attitude estimation methods through experiments, and the results can be used as a reference to be compared with other methods to be developed. In addition, this can help adapt the methods appropriate for a specific underwater application.

Index Terms—Attitude estimation, underwater vehicle, attitude heading reference system, gyro, magnetic field.

I. INTRODUCTION

This paper compares attitude estimation methods that use microelectromechanical systems–attitude heading reference system (MEMS-AHRS) measurement instead of high-end and high-priced inertial measurement units (IMUs). The methods to be compared are for underwater

navigation. Most widely used methods, such as extended Kalman filter (EKF), complementary filter (CF), nonlinear explicit complementary filter (NECF), and a new method called the sine rotation vector (SRV) method, which combines part of NECF and EKF, are compared. The comparison is focused on the statistical analysis of the estimation error: mean, standard deviation, peak to peak, and maximum of the error. A set of measurement data from an experiment in a test tank are used for the application of the methods.

The attitude, which is usually represented by roll, pitch, and yaw, is essential information along with velocity of the vehicles for navigation of underwater vehicles (UVs) or underwater robots. This paper compares attitude estimation methods that use MEMS-AHRS. MEMS-AHRS is cheaper in price, lighter in weight, smaller in volume, and more convenient to use than inertial navigation units that utilize mechanical gyros or fiber optic gyros (FOGs). AHRS provides three measurements: two field measurements of magnetic field and gravity and an angular rate measurement. The AHRS provides these measurements in the instrument coordinate frame. The measured gravity field depends on the roll and pitch of the instrument, and the measured magnetic field depends primarily on yaw. The measurement of the angular rate is useful in calculating incremental changes of the attitude. Since the magnetic field measurement of the AHRS is vulnerable to magnetic interference induced by the vehicle itself and the environment surrounding the vehicle, the estimated yaw based on the AHRS measurement is less reliable than the estimate of roll and pitch.

Interference of the magnetic field is one of the most critical issues when using a magnetometer for attitude estimation. Although many methods have investigated the

estimation of the bias of the magnetic field measurement [1], it is still hard to estimate and compensate for the bias because of the following: the bias and interference depend on environmental aspects, which vary with time and place, and bias is in all directions, that is, it is in the north, east, and Earth-centered directions. The methods to be compared in this research use magnetic field measurements, for which the bias is partially compensated using a Kalman filter (KF).

Attitude estimation has been studied for about a century in the field of aerial and space vehicle navigation. These researches have been adapted and developed for the navigation of UVs. Many of the attitude estimation methods for underwater robots and vehicles use KF, specifically extended KF (EKF), in which the angular rate is used for the prediction of attitude and the gravity and magnetic field are used for correction of the predicted attitude. In the correction stage, the gravity and magnetic field are converted to Euler angles, that is, roll, pitch, and yaw, to calculate the innovation for the correction [2, 3]. The CF method, which utilizes the long-term robustness of the gravity and magnetic field measurement and short-term accuracy of the angular rate, also uses the Euler angles converted from the measurements.

Other methods using unscented Kalman filter (UKF) and cubature Kalman filter (CKF) have also been used for attitude estimation. UKF derives sigma points from a covariance matrix to approximate the probabilistic distribution of state. Sigma points are propagated by a state transition model. The propagated sigma points are transferred to measurement points using a measurement model. These propagated sigma points represent the probability distribution of the predicted state. The sigma points and the measurement points are used to calculate the covariance matrix of the predicted state and predicted measurement. Similar to UKF, CKF uses cubature points to approximate the probability distribution of state variable. CKF also propagates cubature points and calculates the predicted observation by applying the measurement model to the propagated cubature points. Then, it calculates covariance matrices using the propagated cubature points and measurements [4, 5]. UKF has been used for underwater navigation [6]. CKF, which is a more recent development than UKF, is applied for attitude estimation of spacecraft [7, 8, 9].

Approaches that use field measurements represented as the field vector in a rectangular instrument coordinate system without converting to Euler angles are the NECF [10, 11] and SRV method [12]. SRV utilizes the EKF approach, whereas NECF uses the observer approach for attitude estimation.

This paper compares the performances of the four methods: EKF, CF, NECF, and SRV. UKF and CKF are extensions of KF for use with nonlinear state transition models and measurement models. They are generally more suitable to deal with the nonlinearity of the state transition and measurement than EKF; non-Gaussian probability distribution can also be dealt with more appropriately by UKF and CKF than by EKF. Nevertheless, EKF has been widely used for attitude

estimation in underwater applications. Moreover, the performance of EKF is usually comparable to that of UKF and CKF in many applications; therefore, EKF is used for comparison in this research [13, 14]. NECF is one of the widely used methods for attitude estimation for underwater as well as aerial applications [10, 11], and adaptation of NECF is also widespread [15, 16]. SRV is used for comparison since it calculates the SRV from the field measurement to find the innovation that will be used at the correction procedure of EKF application. It takes advantage of using field measurements like NECF and inherits the robustness of the KF approach, which has been proved by a huge amount of variety applications of KF approaches for over fifty years since the KF came into existence in 1960.

Section II describes these methods briefly, Section III compares the performances of the methods through experiments, and Section VI concludes the paper with suggestions for further development of the research.

II. ATTITUDE ESTIMATION METHODS

A. Nomenclature

The notations that are used in this paper are listed below.

- $\boldsymbol{\eta}_1(t)$ Location of a UV at time t in reference coordinate frame;
 $\boldsymbol{\eta}_1(t) = [x(t) \ y(t) \ z(t)]^T$.
- $\boldsymbol{\eta}_2(t)$ Attitude at time t represented by roll, pitch, and yaw of a UV in reference coordinate frame; $\boldsymbol{\eta}_2(t) = [\phi(t) \ \theta(t) \ \psi(t)]^T$.
- $\mathbf{v}_1(t)$ Velocity of a UV at time t in UV coordinate frame; $\mathbf{v}_1(t) = [u(t) \ v(t) \ w(t)]^T$.
- $\mathbf{v}_2(t)$ Angular rate of a UV at time t in the UV coordinate frame;
 $\mathbf{v}_2(t) = [p(t) \ q(t) \ r(t)]^T$.
- $\hat{\mathbf{x}}(t)$ Attitude estimated for the time t ;
 $\hat{\mathbf{x}}(t) = [\hat{\phi}(t) \ \hat{\theta}(t) \ \hat{\psi}(t)]^T$.
- $\mathbf{x}^-(t)$ Attitude predicted for the time t ;
 $\mathbf{x}^-(t) = [\phi^-(t) \ \theta^-(t) \ \psi^-(t)]^T$.
- $\mathbf{a}(t)$ Acceleration measured in the instrument coordinate frame;
 $\mathbf{a}(t) = (a_x(t), a_y(t), a_z(t))^T$.
- $\mathbf{a}_{unit}(t)$ Normalized acceleration measurement;
 $\mathbf{a}_{unit}(t) = (a_x(t), a_y(t), a_z(t))_{unit}^T = \frac{\mathbf{a}(t)}{\|\mathbf{a}(t)\|}$.
- $\mathbf{m}(t)$ Magnetic field measured in the instrument coordinate frame;
 $\mathbf{m}(t) = (m_x(t), m_y(t), m_z(t))^T$.
- $\mathbf{m}_{unit}(t)$ Normalized magnetic field measurement;
 $\mathbf{m}_{unit}(t) = (m_x(t), m_y(t), m_z(t))_{unit}^T = \frac{\mathbf{m}(t)}{\|\mathbf{m}(t)\|}$.
- ${}^w\mathbf{R}_s$ Rotation matrix that converts a vector in the UV coordinate system into a vector in the reference coordinate system. It is represented in terms of ϕ , θ , and ψ of the UV.
- ${}^s\mathbf{R}_w$ Rotation matrix that converts a vector in the reference coordinate system into a vector in the UV coordinate system;

$${}^s\mathbf{R}_w = {}^w\mathbf{R}_s^{-1} = {}^w\mathbf{R}_s^T.$$

B. EKF for Attitude Estimation

EKF is one of the prevalent approaches for attitude estimation. The state $\mathbf{x}(t)$ to be estimated and the measurement $\mathbf{z}(t)$ for the application of EKF consist of roll, pitch, and yaw, as shown in

$$\mathbf{x}(t) = \mathbf{z}(t) = [\phi(t) \quad \theta(t) \quad \psi(t)]^T. \quad (1)$$

To predict the attitude, the differential equation (2), which requires an angular rate measurement, is integrated with time.

$$\begin{aligned} \dot{\phi}(t) &= p(t) + q(t) S\phi(t) T\theta(t) \\ &+ r(t) C\phi(t) T\theta(t) \\ \dot{\theta}(t) &= q(t) C\phi(t) - r(t) S\phi(t) \\ \dot{\psi}(t) &= q(t) \frac{S\phi(t)}{C\theta(t)} + r(t) \frac{C\phi(t)}{C\theta(t)} \end{aligned} \quad (2)$$

In Eq. (2), C , S , and T represent cos, sin, and tan, respectively. $p(t)$, $q(t)$, and $r(t)$ are measured by the AHRS in the sensor coordinate frame. To use Eq. (2) for prediction of attitude at time t_k , the attitude $\hat{\mathbf{x}}(t_{k-1})$, which is estimated at time t_{k-1} , is used.

The gravity and magnetic field measurement is converted to roll and pitch for use in the calculation of innovation in the correction step of the EKF by

$$\begin{aligned} \phi(t) &= \text{atan2}(-a_y(t), -a_z(t)), \\ \theta(t) &= \text{atan2}(a_x(t), \sqrt{a_y^2(t) + a_z^2(t)}). \end{aligned} \quad (3)$$

The magnetic field measurement $\mathbf{m}(t)$ is used to calculate yaw as follows:

$$\psi(t) = \text{atan2}(-{}^w m_y(t), -{}^w m_z(t)), \quad (4)$$

$${}^w\mathbf{m}(t) = [{}^w m_x(t) \quad {}^w m_y(t) \quad {}^w m_z(t)]^T = {}^w\mathbf{R}'_s \mathbf{m}(t).$$

The rotation matrix in Eq. (4) is given in terms of $\phi(t)$ and $\theta(t)$, which are calculated by Eq. (3).

$${}^w\mathbf{R}'_s = \begin{bmatrix} C\theta(t) & S\phi(t)S\theta(t) & C\phi(t)S\theta(t) \\ 0 & -C\theta(t) & -S\phi(t) \\ -S\theta(t) & S\phi(t)C\theta(t) & C\phi(t)C\theta(t) \end{bmatrix}. \quad (5)$$

The EKF method uses the state transition model given by Eq. (2). The measurement model is modeled by an identity matrix since the measurement variable is the same as the state variable as indicated by Eq. (1).

C. SRV Method

The SRV method uses the cross product of two unit vectors to represent the difference of the predicted attitude and reference attitude [12]. SRV combines the attitude errors detected by the gravity and magnetic field measurement using the SRV $\mathbf{r}(t)$ given by

$$\begin{aligned} \mathbf{r}(t) &= \gamma_{-z} \mathbf{r}_{-z}(t) + \gamma_x \mathbf{r}_x(t) \\ &= {}^s\mathbf{R}_w(t) \begin{bmatrix} 0 \\ 0 \\ -1 \end{bmatrix} \\ &\times \mathbf{a}_{unit}(t) \end{aligned} \quad (6)$$

$$\begin{aligned} \mathbf{r}_x(t) &= {}^s\mathbf{R}_w(t) \begin{bmatrix} 1 \\ 0 \\ 0 \end{bmatrix} \\ &\times \mathbf{m}'_{unit}(t) \\ \mathbf{m}'_{unit}(t) &= \begin{pmatrix} \mathbf{m}(t) \\ -\frac{\mathbf{m}(t) \cdot \mathbf{a}(t)}{\mathbf{a}(t) \cdot \mathbf{a}(t)} \mathbf{a}(t) \end{pmatrix}_{unit} \\ \gamma_{-z} + \gamma_x &= 1 \end{aligned}$$

The SRV $\mathbf{r}(t)$ bears the rotation information from the presumed attitude to the measured attitude [12]. $\mathbf{r}_{-z}(t)$ stands for the rotation of the acceleration vector from the Earth-centered gravity direction. $\mathbf{r}_x(t)$ represents the rotation of the magnetic field measurement from the north. $\mathbf{r}(t)$ is the linear combination of $\mathbf{r}_{-z}(t)$ and $\mathbf{r}_x(t)$ and is used to calculate the innovation for the correction stage of EKF. The SRV is converted into Euler angles. The Euler angles converted from SRV are different from those used as innovation in the application of EKF described in Section II.B. The innovation represented in terms of roll, pitch, and yaw in the EKF is calculated by simply subtracting the predicted Euler angles from the Euler angles given by Eqs. (3) and (4).

SRV does not explicitly estimate and compensate for the bias and interference of the magnetic field measurement. Nevertheless, the SRV method reduces the effect of bias and interference. It uses only the northward direction of the magnetic field and ignores the east and Earth-centered direction components. Therefore, it is not affected by bias and interference in these two directions. Likewise, it uses only the Earth-centered direction of acceleration, thus eliminating the interference affecting the acceleration measurement toward the north and east.

D. CF Method

The CF method utilizes the long-term stability of the gravity measurement and magnetic field measurement. To compensate for the short-term instability of these two field measurements, the short-term performance of the angular rate measurement is used. Information by the angular rate measurement is passed through a high-pass filter, whereas information by the magnetic field and acceleration measurement is passed through a low-pass filter. The information from the high-pass filter and that from the low-pass filter are joined together to provide the attitude estimate. In this study, the attitude output from the proprietary CF of the AHRS is also used for comparison with other methods.

E. NECF Method

NECF uses the angular rate, in which the bias is compensated for attitude estimation. It uses the magnetic field and gravity vector for the estimation and compensation of the bias [10, 11]. NECF uses the observer described by Eqs. (7) through (10).

$${}^w\hat{\mathbf{R}}_s = {}^w\hat{\mathbf{R}}_s (\mathbf{v}_2(t) - \hat{\mathbf{b}} + k_p \boldsymbol{\sigma})_x \quad (7)$$

$$\begin{aligned} \hat{\mathbf{b}} &= -k_b \hat{\mathbf{b}} \\ &+ k_b \text{sat}_\Delta(\hat{\mathbf{b}}) \\ &- k_l \boldsymbol{\sigma}, \end{aligned}$$

where $|\hat{\mathbf{b}}(0)| < \Delta$, $\text{sat}_\Delta(\hat{\mathbf{b}}) := \hat{\mathbf{b}} \min(1, \Delta/|\hat{\mathbf{b}}|)$, and

$$\boldsymbol{\sigma} = \sum_{i=1}^n k_i \mathbf{f}_i \times {}^w \mathbf{R}_s^T \mathbf{f}_{oi} \quad (8)$$

In Eq. (8), k_p , k_l , k_b , and k_i denote positive gains, ${}^w \mathbf{R}_s(0) \in SO(3)$, and $\Delta > |\mathbf{b}|$, where \mathbf{b} is the constant bias.

$$\begin{aligned} \mathbf{f}_1 &= \frac{\hat{\mathbf{g}}}{|\hat{\mathbf{g}}|}, \mathbf{f}_{o1} = [0 \ 0 \ -1]^T, \\ \mathbf{f}_2 &= \frac{\hat{\mathbf{m}}_a}{|\hat{\mathbf{m}}_a|}, \mathbf{f}_{o2} = [1 \ 0 \ 0]^T, \end{aligned} \quad (9)$$

$$\hat{\mathbf{g}} = \mathbf{a}(t) - (\mathbf{v}_2(t))_\times \mathbf{v}_1(t) - \dot{\mathbf{v}}_1(t). \quad (10)$$

In Eq. (7), ${}^w \mathbf{R}_s$ represents the rotation matrix, which can be converted to Euler angles and vice versa. $\mathbf{v}_2(t)$ is the angular rate measured by the AHRS. It requires at least two field measurements whose inertial values \mathbf{f}_{o1} and \mathbf{f}_{o2} are known and are not collinear with each other [10, 11, 13]. \mathbf{f}_1 and \mathbf{f}_2 are the measurements corresponding to \mathbf{f}_{o1} and \mathbf{f}_{o2} . In this research, \mathbf{f}_1 is the measured acceleration and \mathbf{f}_2 is the measured magnetic field, which are normalized. It is assumed that the magnetic field north coincides with true north. k_1 and k_2 are the weights to the belief on acceleration and magnetic field measurement. In general, magnetic field measurements are more vulnerable to distortion than acceleration measurements. So, k_1 has a higher value than k_2 . Usually, k_1 is over 0.9 and k_2 is below 0.1, and $k_1 + k_2 = 1$.

Equation (10) describes the compensation of acceleration measurements to calculate pure gravity by subtracting the proper acceleration of motion from the acceleration measured by the AHRS. $\mathbf{a}(t)$ represents the acceleration measured by the AHRS, which includes proper acceleration as well as acceleration due to gravity. $\mathbf{v}_1(t)$ represents the velocity measured by DVL, and $\mathbf{v}_2(t)$ is the angular rate measured by the AHRS. It is assumed that Earth is flat locally, and the North East Down (NED) coordinate frame is inertial in the local workspace, even though the NED is not inertial rigorously.

III. PERFORMANCE EVALUATION THROUGH EXPERIMENTS

The methods are tested using a set of measurement data, which is sampled through an experiment for which a remotely operated UV equipped with an AHRS and a high-end FOG navigates in a test tank. The attitude provided by the high-end FOG is used as a reference to compare the performances of the methods. The error of the estimated attitude from the reference is statistically analyzed using the mean, standard deviation, peak to peak, and maximum of the error. Trajectory estimation

depends on the attitude and the velocity of the vehicle. Although the trajectory error is due to the uncertainty of both the attitude and the velocity, it is regarded that the trajectory estimation error is a partial indication of the performance of the attitude estimation. Thus, analysis on the trajectory error is also included to show the performance of the attitude estimation method indirectly.

The experiment uses an AHRS (LORD MicroStrain 3DM-GX4-25), a FOG (Advanced Navigation, Spatial Fog), and a DVL (Teledyne RD Instruments, Navigator Doppler Velocity Log). DVL measures the velocity of the vehicle in the coordinate frame of the DVL. The velocity from the DVL is used for trajectory estimation after it is converted to the velocity in the NED coordinate frame using the attitude estimate. According to the manual for the AHRS, the gyro bias instability is $10^\circ/\text{hour}$, acceleration noise density is $100 \mu\text{g}/\sqrt{\text{Hz}}$, and magnetometer noise density is $100 \mu\text{Gauss}/\sqrt{\text{Hz}}$ [17]. In case the internal CF is used, the attitude accuracy will be $\pm 0.5^\circ$ in the static status and $\pm 2.0^\circ$ in the dynamic status.

The FOG provides roll and pitch with an accuracy of 0.01° and heading with an accuracy of 0.25° secant latitude if only north seeking is used without the GNSS aid [18]. Since the remotely operated vehicle (ROV) is in the test tank and submerged underwater, GNSS sensing is not available.

The DVL that pings an acoustic signal of 600 kHz from a four-beam Janus array provides a velocity measurement in which the standard deviation of error is 0.3 cm/s at the speed of 1.0 m/s [19]. The standard deviation increases as the speed increases. The DVL can measure the speed when the bottom is within the range of 0.7–90 m from the sensor array.

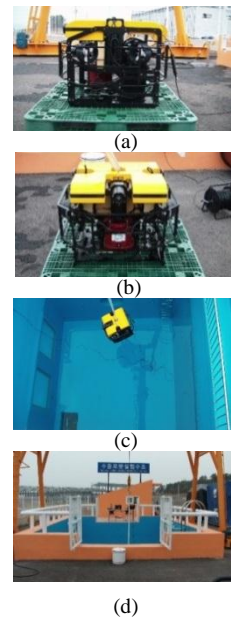


Figure 1. ROV used for the experiment and the test tank. (a) ROV rear view, (b) ROV front view, (c) bird's eye view of the test tank, and (d) side view of the test tank.

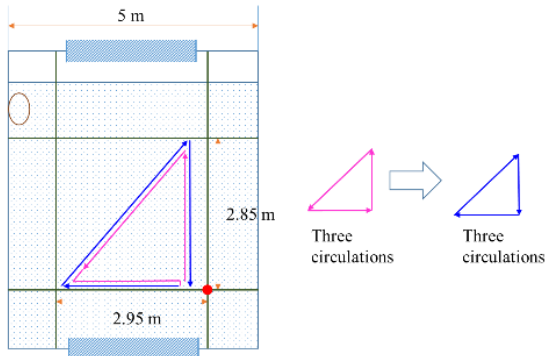


Figure 2. Trajectory of the navigation for the experiment.

An ROV equipped with sensors navigates in a test tank for an hour through a 297 m trajectory. Fig. 1 depicts the test tank and the ROV used for the experiment. Fig. 2 shows the trajectory of navigation. The ROV navigates in a triangular trajectory and is controlled manually to follow the trajectory. Although the triangular trajectory is not precisely traced, it is carefully adjusted so that the final location is the same as the initial location. Therefore, the last location can be used as the ground truth location, which can be used for the evaluation of the trajectory estimation method. The dead-reckoning error at the final location can be a measure of the attitude estimation performance.

The ROV navigates counterclockwise three circulations and turns back and navigates in the reverse direction for three circulations. This navigation repeats five times. Table I shows the mean and standard deviation of the attitude error in roll, pitch, and yaw. In Table I, CF represents the CF algorithm implemented by the authors, and CF-AHRS indicates the algorithm implemented internally for the AHRS. The attitude by CF-AHRS is the attitude output provided by the AHRS itself. Fig. 3 depicts the error in yaw estimate with time, and Fig. 4 depicts the error in roll estimation.

Table II shows the distance error of the estimated location at the final location of the trajectory. Fig. 5 shows the trajectory estimated using the attitude by NECF and the velocity measured by DVL (in blue). Fig. 5 also shows the trajectory calculated using the attitude by FOG (in orange) for comparison. When the NECF was used, the estimated location was found to be 1.372 m away from the true location at the final destination. The deviation was 1.499 m and 2.312 m for the SRV and EKF, respectively. CF and AHRS-CF result in a larger estimation error in location at the destination than NECF, SRV, and EKF. The level of the position error at the destination coincides with the level of the attitude error. Specifically, the standard deviation of yaw error has more relevance with the position error than the mean of yaw error. Although the mean error of roll and pitch of the SRV is worse than that of CF and CF-AHRS, the difference is less than the difference in standard deviation of yaw error. In addition, it is remarkable that although the mean error of yaw of SRV and NECF is larger than that of CF and CF-AHRS, the position error is far better than that of CF and CF-AHRS.

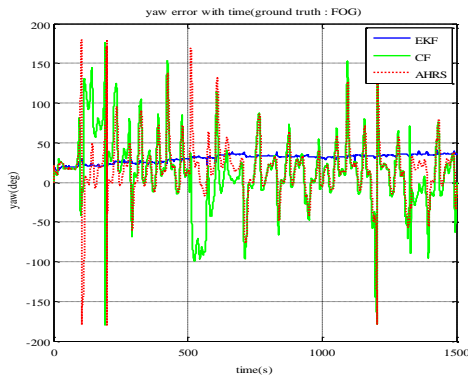
As shown in Figs. 3 and 4 and Tables I and II, the estimation errors in roll and pitch are comparable with each other, whereas the error in yaw estimation shows a remarkable difference. Although the means of attitude error are comparable, the standard deviation of the error shows distinctive differences. In particular, the standard deviation of the yaw error proves that NECF and SRV show an improvement over the EKF and CF. While the mean of the estimation error in yaw for SRV is larger than that for NECF, the standard deviation of the error is less than that of NECF. The mean of the attitude error could be considered as a bias in estimation. This suggests that if bias in estimation can be removed, the SRV will provide a more accurate estimation of yaw. The mean of the estimation errors by CF and CF-AHRS is comparable to that by NECF and less than that of SRV. In addition, the standard deviation of the roll and pitch error by the methods is comparable to that by NECF. However, the standard deviation of yaw error of the CF and CF-AHRS methods is the largest among the methods. From the comparison, it is suggested that the roll and pitch from any of the methods are acceptable. In case of yaw, the use of NECF or SRV is preferable. Furthermore, NECF and SRV would be superior to others if bias in the yaw estimation could be removed. It is supposed that the bias can be removed in two ways: the first is by estimating and compensating the bias in magnetic field measurements and the other is by doing the estimation and compensation with respect to the bias in yaw estimation itself.

TABLE I. STATISTICS OF ATTITUDE ERROR OF THE METHODS.

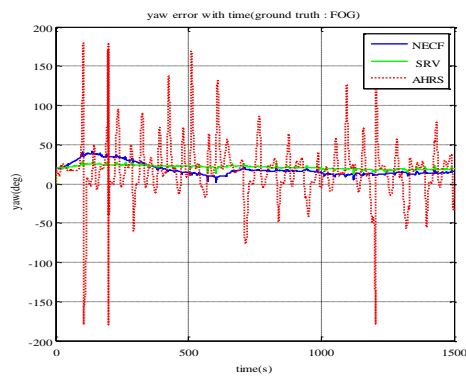
	Mean of error (deg.)			Standard deviation (deg.)		
	Roll	Pitch	Yaw	Roll	Pitch	Yaw
EKF	-0.790	0.207	37.879	0.288	0.257	7.646
CF	-0.393	0.084	16.577	0.261	0.241	44.438
SRV	-1.130	1.150	20.236	0.718	0.721	2.125
NECF	-0.413	0.071	17.616	0.202	0.232	5.593
CF-AHRS	-0.755	0.144	16.907	0.275	0.243	34.017
	Peak to peak (deg.)			Maximum (deg.)		
	roll	pitch	yaw	roll	pitch	yaw
EKF	1.652	1.765	41.756	1.398	0.889	55.56
CF	13.057	5.486	359.48	7.195	3.905	179.84
SRV	3.837	4.204	20.679	2.457	2.195	29.363
NECF	1.811	1.638	39.815	1.597	0.868	41.503
CF-AHRS	1.458	1.481	359.40	1.268	0.112	179.87

TABLE II. POSITION ERROR AT THE FINAL DESTINATION.

	Directional error (m)			Error distance (m)
	x-axis	y-axis	z-axis	
EKF	2.242	0.199	-0.527	2.312
CF	32.032	12.722	0.718	34.473
SRV	1.466	0.170	-0.260	1.499
NECF	1.227	-0.012	0.613	1.372
CF-AHRS	42.939	-7.550	-0.651	43.598

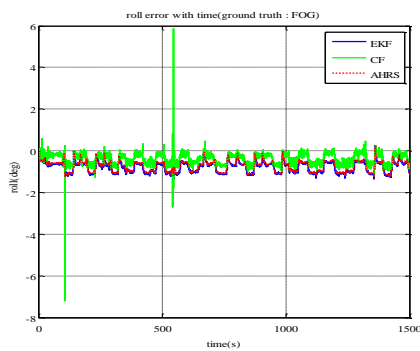


(a)

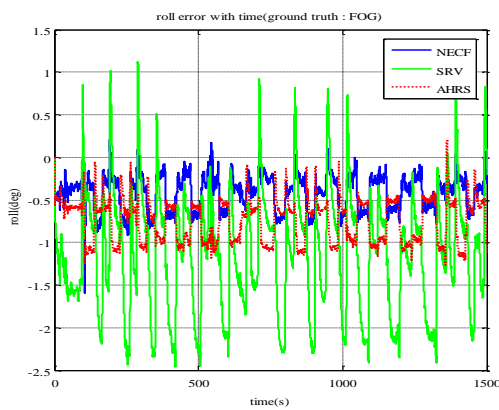


(b)

Figure 3. Error in yaw estimation compared with the yaw measured by FOG. (a) EKF and CF; (b) NECF and SRV.



(a)



(b)

Figure 4. Error in roll estimation compared with the yaw measured by FOG. (a) EKF and CF; (b) NECF and SRV.

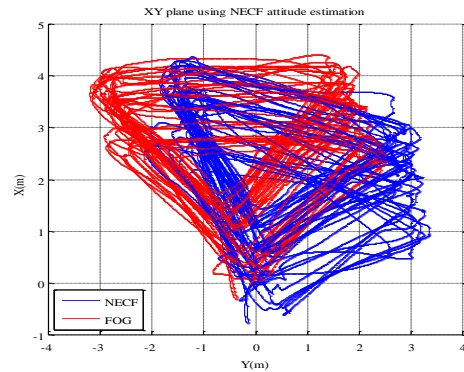


Figure 5. Estimated trajectory using the attitude by NECF.

IV. CONCLUSIONS

This paper presented a comparison of several attitude estimation methods through an experiment. The methods encompass the NECF method, SRV method, EKF, and CF method. In the statistical analysis, methods that use field measurements without conversion to Euler angles exhibit a robust performance. However, it should be noted that the KF application has many variations and the KF used in the paper is just one of the variations [20]. In addition, the performance of an algorithm depends on the parameter values used in each application.

In further research, it is expected that the methods that detect and compensate the distortion in magnetic field measurements be involved in the application of the attitude estimation methods presented in this paper. Another possibility is estimating and compensating the bias in attitude, especially in yaw. There is also a need to investigate the computational expenses for each method to test whether the methods are appropriate for real-time applications. Analysis on robustness against the measurement noise and instability would help choose a proper method because each commercial AHRS exhibits different measurement characteristics in the level of noise and stability.

ACKNOWLEDGMENT

This study was supported by research funds from Chosun University, Korea, 2016.

REFERENCES

- [1] G. Troni and R. M. Eustice, "Magnetometer bias calibration based on relative angular position: Theory and experimental comparative evaluation," in *Proc. 2014 IEEE/RSJ International Conference on Intelligent Robots and Systems (IROS 2014)*, IEEE, pp. 444-450, Sep. 2014.
- [2] J. L. Crassidis, F. L. Markley, and Y. Cheng, "Survey of nonlinear attitude estimation methods," *Journal of Guidance, Control, and Dynamics*, vol.30, no.1, pp. 12-28, Jan. 2007.
- [3] F. L. Markley, "Attitude error representations for Kalman filtering," *Journal of Guidance, Control, and Dynamics*, vol. 26, no. 2, pp. 311-317, Mar. 2003.
- [4] I. Arasaratnam and S. Haykin, "Cubature kalman filters," *IEEE Transactions on Automatic Control*, vol. 54, no. 6, pp. 1254-1269, June. 2009.
- [5] I. Arasaratnam and S. Haykin, "Cubature kalman smoothers," *Automatica*, vol. 47, no. 10, pp. 2245-2250, Oct. 2011.

- [6] N. Y. Ko, S. W. Noh, and H. T. Choi, "Simultaneous estimation of sea level and underwater vehicle location," in *Proc. Oceans 2014-Taipei*. IEEE, Taipei, April 7-10, 2014.
- [7] X. Tang, J. Wei, and K. Chen, "Square-root adaptive cubature Kalman filter with application to spacecraft attitude estimation," in *Proc. 2012 15th International Conference on Information Fusion (FUSION)*, Singapore, July 9-12, 2012.
- [8] X. Tang, Z. Liu, and J. Zhang, "Square-root quaternion cubature Kalman filtering for spacecraft attitude estimation," *Acta Astronautica*, vol.76, pp.84-94, July-Aug. 2012.
- [9] H. Pesonen and R. Piché "Cubature-based Kalman filters for positioning," in *Proc. 2010 7th Workshop on Positioning Navigation and Communication (WPNC)*, Dresden, Mar 11-12, 2010.
- [10] M. D. Hua, K. Rudin, G. Ducard, T. Hamel, and R. Mahony, "Nonlinear attitude estimation with measurement decoupling and anti-windup gyro-bias compensation," in *Proc. 18th IFAC World Congress*, Elsevier Ltd, pp. 2972-2978, Jan. 2011.
- [11] R. Mahony, T. Hamel, and J. M. P. flimlin, "Nonlinear complementary filters on the special orthogonal group," *IEEE Transactions on Automatic Control*, vol. 53, no. 5, pp. 1203-1218, Aug. 2008.
- [12] N. Y. Ko, S. Jeong, and Y. Bae, "Sine rotation vector method for attitude estimation of an underwater robot," *Sensors*, vol. 16, no. 8, pp. 1213-1230, Aug. 2016.
- [13] G. Troni and L. L. Whitcomb, "Preliminary experimental evaluation of Doppler-aided attitude estimator for improved Doppler navigation of underwater vehicles," in *Proc. 2013 IEEE International Conference on Robotics and Automation (ICRA)*, IEEE, pp. 4134-4140, May. 2013.
- [14] M. R. Morelande and A. F. Garcia-Fernandez, "Analysis of Kalman filter approximations for nonlinear measurements," *IEEE Transactions on Signal Processing*, vol. 61, no. 22, pp.5477-5484, Nov. 2013.
- [15] B. Allotta, R. Costanzi, F. Fanelli, N. Monni, and A. Ridolfi, "Single axis FOG aided attitude estimation algorithm for mobile robots," *Mechatronics*, vol. 30, pp. 158-173, Sep. 2015.
- [16] R. Costanzi, F. Fanelli, N. Monni, A. Ridolfi, and B. Allotta, "An attitude estimation algorithm for mobile robots under unknown magnetic disturbances," *IEEE/ASMET Transactions on Mechatronics*, vol. 21, no. 4, pp. 1900-1911, Aug. 2016.
- [17] *Data Sheet 3DM-GX4-25™*, LORD Corporation, Document 8400-0060 Revision B, 2016.
- [18] *Spatial FOG Reference Manual Advanced Navigation*, Ver 2.0, Oct. 2014.
- [19] *NAVIGATOR Doppler Velocity Log (DVL) Technical Manual*, Teledyne RD Instruments, Inc.P/N 957-6172-00, Feb. 2013.
- [20] Fred Daum, "Nonlinear filters: Beyond the Kalman filter," *IEEE Aerospace and Electronic Systems Magazine*, vol. 20, no. 8, pp. 57-69, Aug. 2005.



Nak Yong Ko obtained his Ph.D., M.Sc., and bachelor's degree in the field of robotics from the Dept. of Control and Instrumentation Eng., Seoul National University, Seoul, Korea, in 1993, 1987, and 1985, respectively. His major researches include navigation, collision avoidance, and motion planning, all in robotics. He has been with the Department of Electronic Eng., Chosun University, Gwangju, Korea, since 1992 as a Professor.

He worked as a Visiting Research Scientist at the Robotics Institute, Carnegie Mellon University, Pittsburgh, PA, USA, for the years 1997-1998 and 2004-2005. Professor Ko is a member of IEEE Robotics and Automation Society and the Institute of Control, Robotics, and Systems, Korea.

Seokki Jeong obtained his M.Sc. degree from the Dept. of Control and Instrumentation Eng., Chosun University, Gwangju, Korea, in 2013, after graduating from the Dept. of Electronic Eng., Honam University, Gwangju, Korea, in 2011. He worked on localization and pose estimation of mobile robots and underwater vehicles. He has been working at Redone Technologies Co., Ltd., Jeonnam, Korea, in the field of mobile robot navigation, since 2017. Mr. Cheong is a member of Korea Robotics Society.



Hyun-Taek Choi received his B.Sc., M.Sc., and Ph.D. degrees from Hanyang University, Seoul, Korea, in 1991, 1993, and 2000, respectively. He joined the Korea Research Institute of Ships and Ocean Engineering (KRISO) in 2003, after working for Korea Telecom and ASL, University of Hawaii, as a Postdoc. He has been leading several projects related to underwater robotic applications, such as underwater robots (both ROV and AUV), advanced control and navigation,

recognition using optic cameras and sonar, and robot intelligence. Dr. Choi is a member of IEEE, Robotics and Automation Society, and Korea Robotics Society.

Yong Seon Moon graduated from Chosun University, Gwangju, Korea, with Ph.D., M.Sc., and bachelor's degrees in 1989, 1985, and 1983, respectively. His major researches include networks of motion and motion planning, all in robotics. He has been a Professor at the Department of Electronic Eng., Sunchon National University, Suncheon, Korea, since 1992. He worked as a Visiting Research Scientist at Pennsylvania State University, USA, for the years 1999-2000. Professor Moon is a member of the Institute of Control, Robotics, and Systems, Korea.